Indian Journal of Fundamental and Applied Life Sciences ISSN: 2231– 6345 (Online)
An Open Access, Online International Journal Available at www.cibtech.org/sp.ed/jls/2016/02/jls.htm
2016 Vol. 6 (S2), pp. 304-314/Seif et al.
Research Article

MORPHORADITION OF ALVAND HEIGHTS AND ITS RELATION WITH QUATERNARY GLACIAL EFFECTS

***Abdollah Seif[1], Ali Bazvand[2] and Sina Solhi[2]**
[1]Department of Geomorphology, School of Geographical Sciences and Planning
[2]Department of Geomorphology, Isfahan University
**Author for Correspondence*

ABSTRACT
Radiation energy has been the most important input energy to all systems including geomorphic systems of Earth. Calculation of radiation energy is conducted through different equations and formulas and is most calculable for horizontal surfaces. Morphoradition model has been used in this study to modeling rough surfaces and interfering Earth topography and its relation with distribution of radiation energy. After preparing Morphoradition maps of Alvand (Hamedan, Iran) Heights from Digital Elevation Modelswith resolution of 10 m, the obtained results were compared to Quaternary glacial effects of Alvand. Results indicate that there is a significant coordination between positions of form and place of glacial effect (glacial cirques and valleys) and diffusion of energy generated from Morphoradition Model of Alvand Heights from the perspective of physical parameters and radiation.

Keywords: *Morphoradition, Alvand Mountainous, Glacial Cirque and Valley, Quaternary, Radiation Duration*

INTRODUCTION
Solar radiation is the main source of energy through Earth planet and is the main factor that controls life and weather of Earth. Solar energy determines pressure and humidity of Earth through controlling temporal and spatial distribution and temperature of Earth. Sun can be considered as a black body that continuously radiates. Total radiation energy of black body is calculated based on Stefan Boltzmann Law (Kaviani & Alijani, 2003).
It is assumed that input energy into all natural and vital systems of earth planet is solar radiation energy and solar energy flow has created all morphogenic systems of earth surface. Accordingly, the importance of radiation energy in geomorphology science is determined. Distribution level of radiation energy on earth surface, which is originated from some factors including amount of solar radiation, the distance from the radiating source, latitude, axial rotation and orbital speed and uneven shapes such as slope, aspect and elevation, is the start point of changes and differences through earth surface. Accordingly, radiation differences would lead to temperature differences and distribution of globe temperature; globe temperature effects on pressure changes on earth surface and these factors directly effect on winds breezing and would determine climate system of earth. Finally, climate system can incredibly control morphologic and erosional systems and determine type of wind, water and glacial morphology and erosion in each place. Then, continuous changing loops of hydrologic and pedogenic systems are affected. The result of these effects can be observed through creation, change and survival of biologic system that are the main part of human life. The relevant studies to the radiation energy should be evaluated based on natural or morphologic systems or perspective of earth morphology due to the direct and indirect effects of this energy on human and human activities. Radiation energy as a new and clean energy can be used also to establish clean and without pollution power planets. This study has been conducted to estimate radiation energy through a complete morphologic system with high accuracy since scientific morphologic communities have les considered uneven shape of the Earth or the same earth morph in their studies.
Seif *et al.*, (2014) have conducted studies of earth radiation about mountainous mass of Eqlid and analyzed its relation with morphologic transformations. Many of researchers have studies energy changes and its effects on permanent snowlines and natural glaciers. Studies conducted by Hugeh Drone *et al.*, (1974) in Shirkooh of Yazd, Iran indicate the presence of old glaciers topography at an altitude of 3200

meters of this mountain. The remained glacial moraines at altitudes of 1800 and 2800 meters demonstrate two glacial eras in this area (Hugeh Drone, 1978). Ramesht (2002) is another researcher who has recently searched about glaciers of central Iran and has confirmed the conducted studies by some scientists such as Hugeh Drone and Kohle. He has studied glaciers at altitude of 1600 meters in several areas of central Iran including Zofreh, Shirkooh, etc. with emphasize on geomorphic evidences and erosional effects and published unique pictures of caught socks in Mehriz area of Yazd, Iran, in about altitude of 1650 meters and observed ice tabs coming down to plain lands. Recently, Dehghanpoor (2010) has conducted studies about glaciers of Shirkuh and explained the effects of uneven direction on glacial erosional systems. The present study has done radiation calculations of mountainous mass of Alvand. The studies area has been so determined to cover all ranges of mountainous mass in order to detect radiation situation through different directions and show its effects on adjacent areas. The total receipt of incoming solar radiation on a given slope is strongly controlled by aspect, thereby explaining the tendency for many glaciers and cirques globally to have pole-ward orientations (Evans, 1977). Specifically, total solar radiation in the Northern Hemisphere is lowest on north-facing slopes; and on south-facing slopes in the southern hemisphere. This pattern results in lower air temperatures on pole-ward-facing slopes (Andrews, 1971; Evans, 1977), where the melting of cumulated snow and ice is therefore limited, and glaciers have a tendency to develop (Coleman *et al.*, 2009). By contrast, equator-facing slopes receive high levels of total insolation, and are therefore climatically unfavorable for glacier development. This results in significant contrasts between the number of north and south-facing glaciers and cirques in many areas globally (Evans, 1977). The strength of aspect-related contrast in the total receipt of direct solar radiation received on particular slopes is greatest in areas of steep topography and, most importantly, in regions characterized by clear skies during the ablation season, since clouds limit the total receipt of direct solar radiation at the Earth surface (Evans, 1977; Nelson, 1998). This has led some to infer that where cirque aspects show a particularly strong pole-ward bias, former cirque glaciers likely developed under comparatively dry and, therefore, cloud-free ablation season conditions (Evans, 1977, 1990, 2006). Arguably though, an even stronger indication of cloud-free conditions is when cirques (and glaciers) are found to have a NNE orientation in the Northern hemisphere, or SSE in the Southern hemisphere (Andrews and Dugdale, 1971; Trenhaile, 1976; Embleton and Hamann, 1988). Specifically, under cloud-free ablation season conditions, NNE-facing slopes in the Northern Hemisphere, and SSE-facing slopes in the Southern Hemisphere receive much of their direct solar radiation in the morning, when air temperatures are relatively low (Evans, 1977, 2006). This limits ablation, and thereby favors glacier survival and associated cirque development. By contrast, on slopes that receive much of their direct solar radiation later in the day (e.g. on NW-facing slopes in the Northern Hemisphere), air temperatures are higher, and ablation is therefore increased, limiting glacier survival and cirque development (Evans, 2006). In cloudy environments, or where there is convective afternoon cloudiness (common in tropical climates), these diurnal variations in temperature are reduced, and the propensity for glaciers, and thereby cirques, to face NNE and SSE (in the Northern and Southern Hemispheres, respectively) diminishes (Evans, 1977). As a result of these trends, cirque aspect has been used as a proxy for former cloudiness (e.g., Evans, 1990, 2006; Barr and Spagnolo, 2013). This is particularly useful, since palaeo cloud-cover is a climatic variable for which there are few other indicators (Evans, 2006).

MATERIALS AND METHODS

The study area belongs to Alvand Heights of Hamedan, Iran. Alvand Heights: Alvand Mountain with direction of Northwest-Southeast and (length of 48 degrees 13 minutes 48 degrees and 38 minutes East) and (34 degrees 13 minutes to 34 degrees and 53 minutes north) is located in bar Urmia Dokhtar and its highest peak with an altitude of 3580 meters, that is called “Gholeh” is a glacier (Sahab Geographical Institution, 1992).

An uneven geometry was needed to calculate radiation of Alvand Mountain with a morphologic system. A spatial geometry of uneven shape shows the rate and direction of the slope as well as the height. Therefore, morphologic model of DEM (Digital Elevation Model) in order to eliminate the needs in this

field. In this regard, four radiation parameters have been applied as the bases of analysis in order to describe radiation status of area.

Calculation of Direct Radiation

Direct radiation is radiation of solar short wave that radiates to the earth surface when the sun is top of the horizon line during day so that solar beams would directly radiate to earth. To calculate the direct radiation on Alvand Mountain, the period that sun is on top of the sky (through interfering latitude of area) is divided into half an hour sectors called Sun Sectors then, the direct radiation is calculated in accordance with the placement of sun in each of these Sun Sectors. Removal rate of radiation wavelength or Atmospheric Attenuation was calculated based on the altitude of each point and thickness of the atmosphere and input energy was considered as constant solar energy and interfered into the calculation. These operations have been calculated for have been calculated. The following formulas have been applied to calculate the direct radiation to the area:

(1) $Dirtot = \Sigma Dir\ \theta,\alpha$

(2) $Dir\theta,\alpha = SConst \times \tau m(\theta) \times SunDur\theta,\alpha \times SunGap\theta,\alpha \times \cos(AngIn\ \theta,\alpha)$

In which:

SConst is solar constant radiation considered within average distance between Earth and Sun outside of Atmosphere. The rate of solar constant has been variable in a range of 1338 to 1368 WM-2.

T is atmospheric transition rate considered averagely for entire range domain.

m (θ) is light transmission coefficient calculating in accordance with zenith distance between distance parameters of zenith and height above sea level.

SunDurθ,α is duration of each Sun Sector that is under direct radiation. Hourly and daily intervals that are half an hour and one day are considered in calculations.

SunGapθ,α is the gap rate of Sun Sectors in the sky.

AngInθ,α is angle radiation of sun toward earth surface.

The following formula has been applied to calculate AngInθ, α.

(3) $AngIn\theta,\alpha = \arccos[\cos(\theta)\times\cos(Gz)+\sin(\theta)\times\sin(Gz)\times\cos(\alpha-Ga)]$

In which, Gz and Ga are angles of surface zenith and azimuth.

According to formula (1), direct radiation is equal to total calculated direct radiation for each SunMap Sector and the radiation amount of each sector is calculated through formula (2). Calculations of direct radiation have been done for one year through study area. The map of direct radiation to the surface of Alvand Mountain is demonstrated in Figure 1.

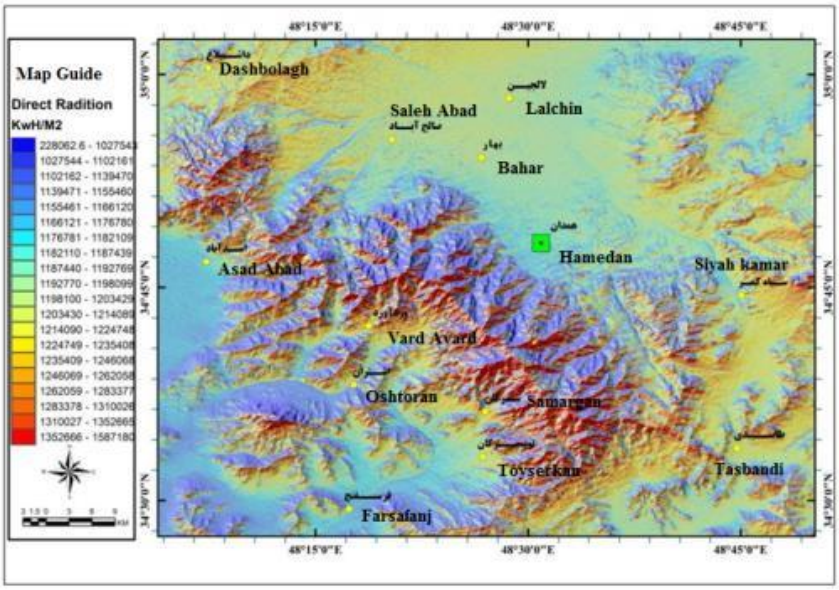

Figure 1: Map of Direct Radiation over Surface of Alvand Mountain per KWh/M2

Analysis of Cross-Section Profile of Direct Radiation over Alvand Mountain

The radiation status of Alvand Height has been investigated through illustration of cross-section profile of Alvand Heights. The effects of glacial cirques can be seen through a wide area in which, the profile of radiation energy is faced a sudden attenuation [Figure 3]

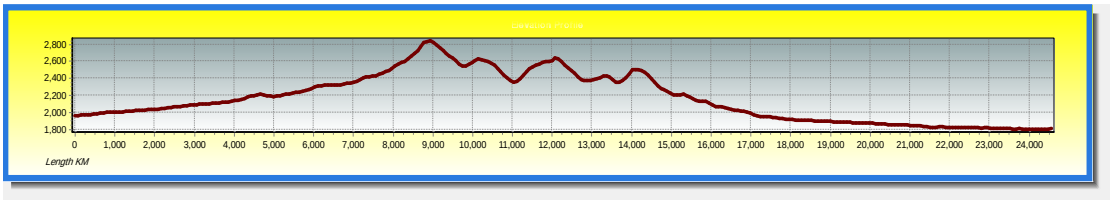

Figure 2: Cross Elevation Profile of Western Alvand Heights

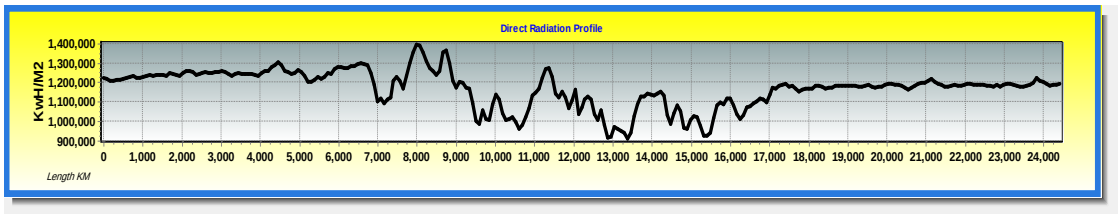

Figure 3: Cross Profile of Direct Radiation over Western Alvand Heights – Similar Path as Figure 2

Duration of Direct Radiation

The more the duration of sun radiation is, the more energy will absorb the Earth. In fact, duration of radiation points out the day duration. Earth's rotation around its axis, would cause each point of earth to be in darkness or in lighting for a period in each full rotation of earth. Day duration of each place is the period in which, that place is in lighting. The big circle shows lighting (Kaviani & Alijani, 2003).

In this study, the duration of direct radiation to the study area has been calculated based on hour for one year presented in frame of distribution map. Latitude of the region as a day duration indicator and uneven shape and morph of the earth as an effective factor have been considered to calculate the duration of direct radiation.

Calculation of Diffused Radiation

It would be necessary to calculate diffused radiation energy in order to analyze energy in study region. As it is known, if diffused radiation is not through the environment and or its amount is near to zero in accordance with theoretical physics then the energy and temperature differences will be high between shade and sunlight so that the vital systems will be disturbed. Therefore, high effects of diffused radiation on natural and unnatural systems or ecosystems can be percept. UOS Model (Uniform Overcast Sky) has been applied to calculate diffused radiation energy.

(4) $Dif\theta,\alpha = Rglb \times Pdif \times Dur \times SkyGap\theta,\alpha \times Weight\ \theta,\alpha \times \cos(AngIn\ \theta,\alpha)$

In which:

Rglb is normal global radiation that formula (5) has been applied to calculate normal global radiation.

(5) $Rglb = (SConst\ \Sigma\ (\tau m(\theta)\ )\ )/\ (1 - Pdif)$

In which:

Pdif is diffusion rate of radiation that is usually between 0/2 for low cloudiness rate and 0/7 for high cloudiness rate. This rate has been equal to 0/3 for study region in accordance with arid and semi-arid climate of region.

Dur is duration that is considered equal to half an hour in this process.

$SkyGap\theta,\alpha$ is gap rate for each Sun Sector.

Weight θ,α is the ratio of diffused radiation generated from one Sun Sector of sky to total Sun Sectors.

Formula (6) has been applied to calculate Weight θ,α

(6) $Weight\ \theta,\alpha = (\cos\theta 2 - \cos\theta 1) / Divazi$

In which, θ1 and θ2 have been the range of zenith in sky sectors and Divazi has been azimuthal deviation of sky.
AngInθ,α is radiation angle between the center of radiation sector and radiation surface. According to formula (7), the diffused radiation energy is obtained from total of diffused radiation for each radiation sector.
(7) Diftot = ΣDif θ,α
According to the mentioned formulas, the relevant map to calculated diffuse radiation over Alvand Mountain has been illustrated in Figure 4.

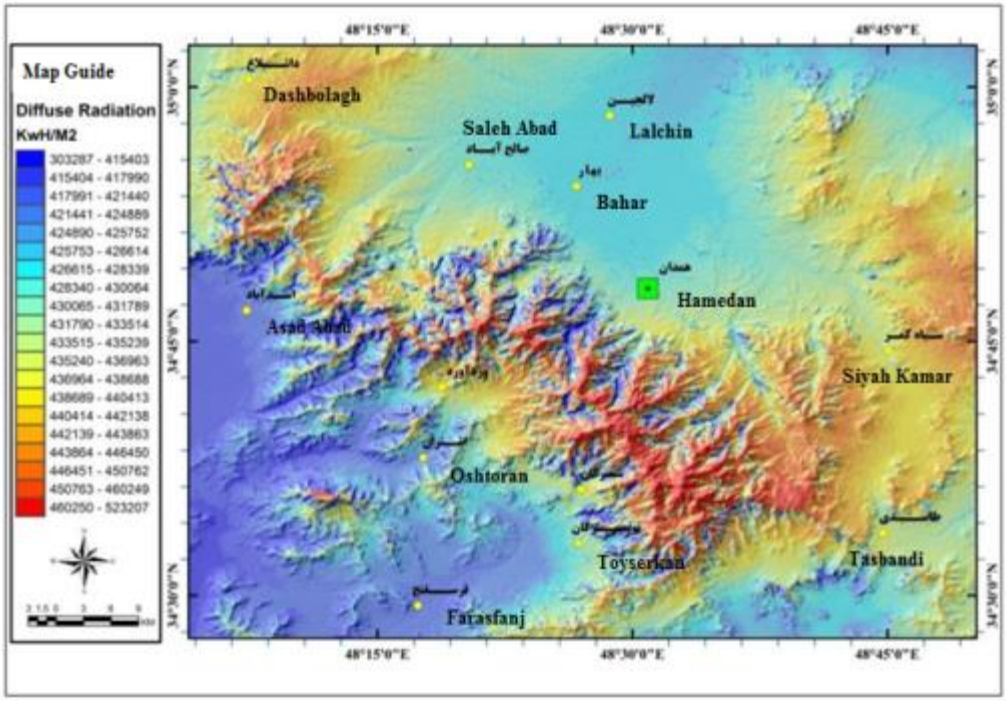

Figure 4: Map of Diffuse Radiation over Alvand Mountain [ONLY USE ENGLISH WORDS, LETTERS AND NUMBERS]

This map depicts diffuse radiation of area that its minimum is equal to 303287 Kwh/m2 through directions of north and west and it maximum is equal to 523207kwh/m2 through southern and eastern ranges through a year. Another important point of this figure is that diffuse radiation amount over flat surfaces is less than uneven surfaces. This matter is related to physics principles so that a flat object will diffuse less the radiated energy to itself while an uneven surface will diffuse more amount of radiation. Accordingly, it can be found that there is a high difference between diffuse radiations through two directions of mountain range.

Analysis of Cross-Section Profile of Diffuse Radiation over Alvand Mountain

Radiation status of mountainous mass of Alvand has been assessed throw illustrating cross-section profile of Alvand Heights. The effects of glacial cirques can be seen through an extensive range when radiation profile is faced a sudden attenuation. This matter has been demonstrated in figure 6.

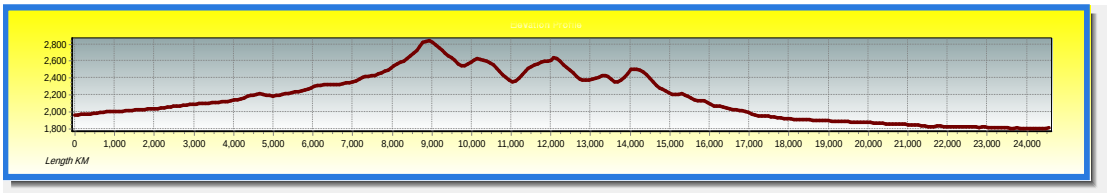

Figure 5: Cross Elevation Profile of Alvand Western Heights

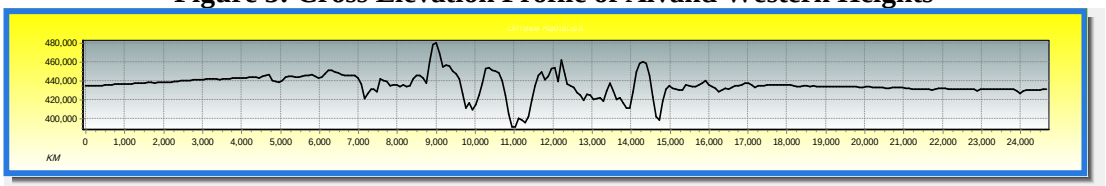

Figure 6: Cross Elevation Profile of Diffuse Radiation over Alvand Western Heights

Global Solar Radiation

Global radiation is equal to total of direct and diffuse radiation of all Sun Sectors. Global radiation has been calculated based on formula (8). Global radiation shows the radiation status of area through a comprehensive way. Global radiation is illustrated in figure 7.

(8) $Global_{tot} = Dir_{tot} + Dif_{tot}$

RESULTS AND DISCUSSION

Direct radiation map [Figure 1] shows that there is a big difference between southward and northward aspects of Alvand Heights. Diffuse Radiation map [Figure 4] shows that convex surfaces got more diffuse radiation energy but concave surface that is matched with valley floor had less diffuse energy. Global radiation map [Figure 7] shows that generally there is a clear deference between northward and southward aspect in Alvand height. Cross section of elevation in Alvand Height had compared with cross section of direct radiation [Figure 2 and 3] as there is notable loss in direct radiation at the northward aspects. Cross section of elevation and similar path of cross section of diffuse radiation [Figure 5 and 6] has also similar loss at northward aspects.

Cross profile of Global Radiation [Figure 9] shows that there is a loss variation in northward aspects. The relation between global radiation and slope direction [Figure 10] shows that there is a significant increase in global radiation at aspects located in 150 up to 200 degree from north. A significant relationship between low energy aspects and location of glacial indicators such as glacial cirques and valleys is detectable [Figure 12].

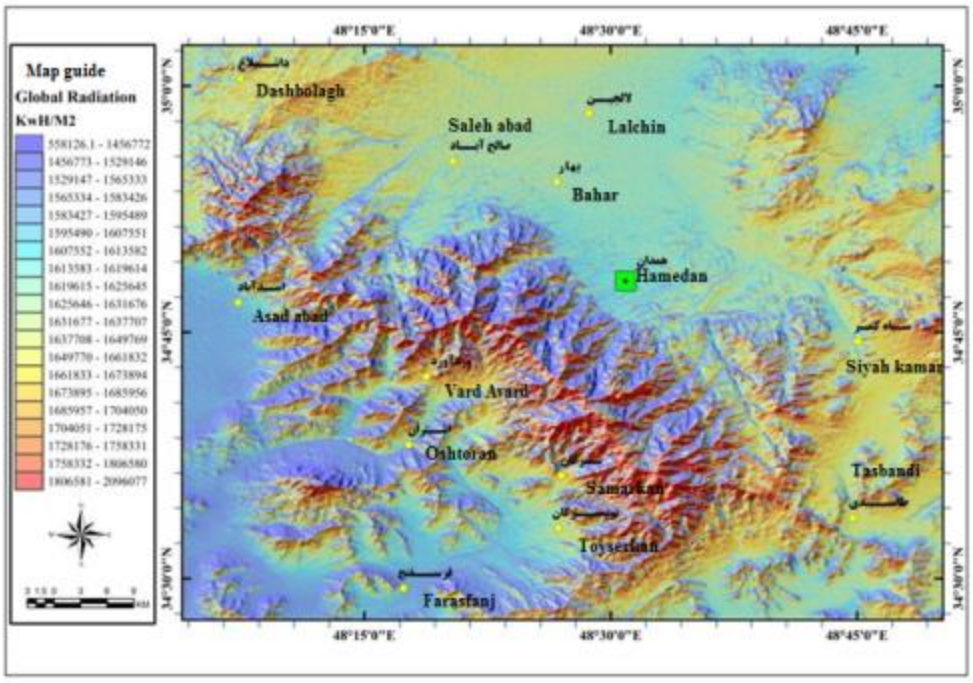

Figure 7: Map of Global Radiation over Mountainous Mass of Alvand

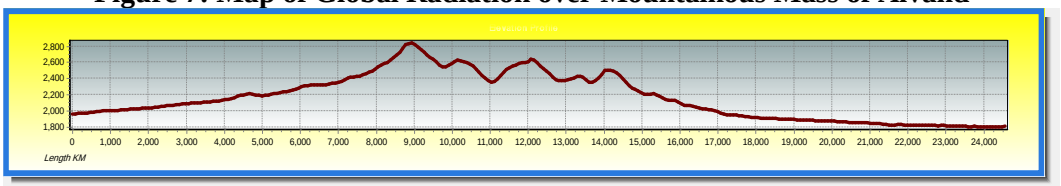

Figure 8: Cross Elevation Profile of Western Heights of Alvand

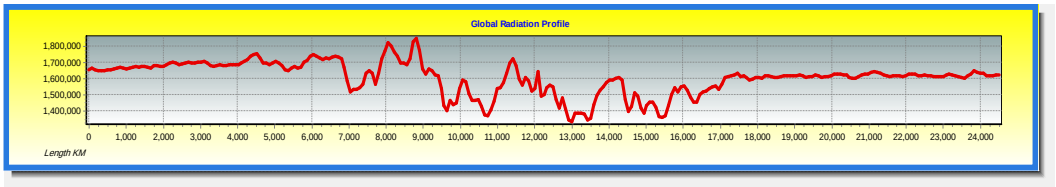

Figure 9: Cross Elevation Profile of Global Radiation over Western Heights of Alvand

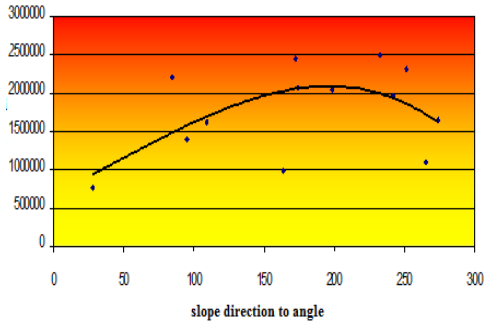

Figure 10. The Relation between Global Radiation and Slope Direction

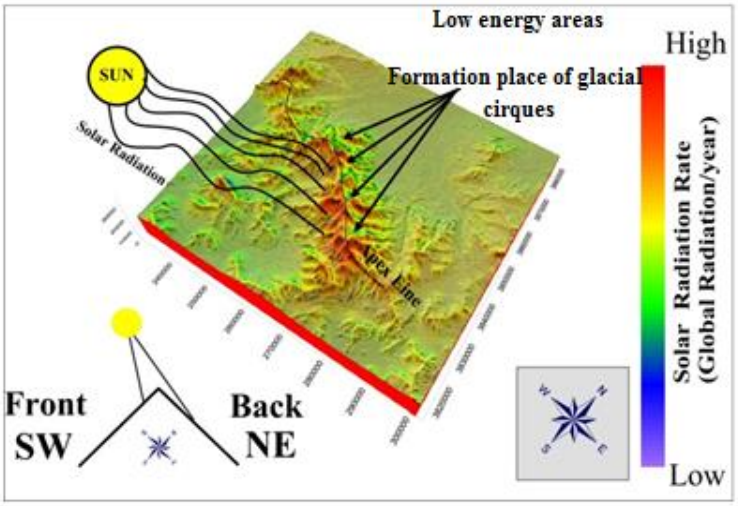

Figure 11. 3D Morphordition of Alvand Heights from the Standpoint of Radiation, Physical Parameters, and Glacial Effects

Figure 12: Situation of Glacial Cirques of Alvand

Conclusion

According to physical and radiation parameters, there is a significant coordination between situation, shape and placement of quaternary glacial effects (glacial cirques and valleys) and obtained maps of Morphoradition Model of Alvand heights. Radiation energy creates thermal, erosional and energy differences and fluctuations through uncoordinated diffusion so that these differences can be observed through heights during a period. Some parts of these effects are on the valleys, cirques and semi-cirques of mountainous mass. Of course, there another effective parameters in study altitudinal mass (Alvand) such as direction of moisture supply, overall climate patterns and direction of rain systems' collision. However, these conditions sometimes act in inverse direction. Comparison and study of Thermal layers of the Earth's surface obtained from satellite data and ground stations as well as its compliance with the albedo fluctuations of the Earth's surface can be an effective step in the completion of the issue.

Table 1: Information of Cross-Section Profile of Direct Radiation

Global Radiation Index	Value
Start Position	256028E3841549 N
End Position	276773 E3854419 N
Start Radiation	1219880 wH/M2
End Radiation	1189019 wH/M2
Straight-Line Distance	24.4 Km
3D Distance on Surface	6119.3 KM
Vertical Difference (Start to Finish)	30860 wH/M2
Minimum Radiation on Path	897995 wH/M2
Maximum Radiation on Path	1409715 wH/M2
Azimuth	56° 40' 0.2"

Table 2: Direct Radiation Indices

Global Radiation Index	Value
Min Radiation	262397 wh/M2
Max Radiation	1563991 wh/M2
Average Radiation	1192050 wh/M2
Mode Radiation	1197227 wh/M2
Radiation Standard Deviation	84550 wh/M2
Radiation Max Slope	89.99°
Radiation Average slope	89.43°
Slope Radiation Standard Deviation	0.86794722°

Table 3: Information of Cross-Section Profile of Direct Radiation Duration

Global Radiation Index	Value
Start Position	256028E3841549 N
End Position	276773 E3854419 N
Start Height	3685.324 wh/M2
End Position	3836.858 wh/M2
Straight-Line Distance	24.4 Km
3D Distance on Surface	32.262Km
Vertical Difference (Start to Finish)	151.5 wh/M2
Minimum Radiation on Path	2512 wh/M2
Maximum Radiation on Path	3855 Kwh/M2

Azimuth	56° 40' 0.2"

Table 4: Statistical Information of Direct Radiation Indices in Study Region

Global Radiation Index	Value
Min Radiation	1216.574 wh/M2
Max Radiation	3962.758 wh/M2
Average Radiation	3672.854 wh/M2
Mode Radiation	3828.3 wh/M2
Radiation Standard Deviation	230.18569 wh/M2
Radiation Max Slope	86.52°
Radiation Average slope	28.25°
Slope Radiation Standard Deviation	21.202831°

Table 5: Information of Cross Profile of Diffuse Radiation

Global Radiation Index	Value
Start Position	256028E3841549 N
End Position	276773 E3854419 N
Start Height	434200 wh/M2
End Position	430277 wh.M2
Straight-Line Distance	24.4 Km
3D Distance on Surface	987 Km
Vertical Difference (Start to Finish)	-3923.4 wh/M2
Minimum Radiation on Path	385698 wh/M2
Maximum Radiation on Path	482212 wh/M2
Azimuth	56° 40' 0.2"

Table 6: Statistical Information of Indices of Diffuse Radiation through Study Area

Global Radiation Index	Value
Min Radiation	328885.781 Kwh/M2
Max Radiation	519979.25 wh/M2
Average Radiation	432248.5 wh/M2
Mode Radiation	426966 wh/M2
Radiation Standard Deviation	11982.967 wh/M2
Radiation Max Slope	89.92°
Radiation Average slope	79.64°
Slope Radiation Standard Deviation	11.923248°

Table 7: Information of Cross Profile of Global Radiation

Global Radiation Index	Value
Start Position	256028E3841549 N
End Position	276773 E3854419 N
Start Height	1650221 Wh/M2
End Position	1623565Wh/M2
Straight-Line Distance	24.4 Km
3D Distance on Surface	7066 Km
Vertical Difference (Start to Finish)	-26656.1 Wh/M2
Minimum Radiation on Path	1305413Wh/M2
Maximum Radiation on Path	1843827Wh/M2

Azimuth	56° 40' 0.2"

Table 8: Statistical Information of Indices of Global Radiation through Study Area

Global Radiation Index	Value
Min Radiation	595730.188 Wh/M2
Max Radiation	2051854.625 Wh/M2
Average Radiation	1624299.125 Wh/M2
Mode Radiation	1625455.875 Wh/M2
Radiation Standard Deviation	89118.457 Wh/M2
Radiation Max Slope	89.99°
Radiation Average slope	89.43°
Slope Radiation Standard Deviation	0.87463897°

REFERENCES

Andrews JT (1971). Quantitative analysis of the factors controlling the distribution of corrie glaciers in Okoa Bay, East Baffin Island: (with particular reference to global radiation). In: Morisawa, M. (edition), Quantitative Geo-morphology: Some Aspects and Applications. *Proceedings of the 2nd. Geomorphology Symposium*, Binghamton, State University of New York 223–241.

Andrews JT and Dugdale RE (1971). Late Quaternary glacial and climatic history of northern Cumberland Peninsula, Baffin Island, NWT, Canada. Part V: factors affecting corrie glacierization in Okoa Bay. *Quaternary Research* **1** 532–551.

Barr ID and Spagnolo M (2013). Palaeoglacial and palaeoclimatic conditions in the NW Pacific, as revealed by a morphometric analysis of cirques upon the Kamchatka Peninsula. *Geomorphology* **192** 15–29.

Coleman CG, Carr SJ and Parker AG (2009). Modelling topoclimatic controls on palaeoglaciers: implications for inferring palaeoclimate from geomorphic evidence. *Quaternary Science Reviews* **28**(3) 249–259.

Embleton C and Hamann C (1988). A comparison of cirque forms between the Austrian Alps and the Highlands of Britain. *Zeitschrift für Geomorphologie. Supplementband* **70** 75–93.

Evans IS (1977). World-wide variations in the direction and concentration of cirque and glacier aspects. *Geografiska Annaler Series A Physical Geography* **59**(3/4) 151–175.

Evans IS (1990). Climatic effects on glacier distribution across the southern Coast Mountains, B.C., Canada. *Annals of Glaciology* **14** 58–64.

Evans IS (2006). Local aspect asymmetry of mountain glaciation: a global survey of consistency of favoured directions for glacier numbers and altitudes. *Geomorphology* **73**(1) 166–184.

Fu P (2000). A Geometric Solar Radiation Model with Applications in Landscape Ecology. Ph.D Thesis, Department of Geography, University of Kansas, Lawrence, Kansas, USA.

Fu P and Rich PM (2000). *The Solar Analyst 1.0 Manual*, (Helios Environmental Modeling Institute (HEMI), USA).

Fu P and Rich PM (2002). A Geometric Solar Radiation Model with Applications in Agriculture and Forestry. *Computers and Electronics in Agriculture* **37** 25–35.

Kaviani MR and Alijani B (2003). Applied principles of hydro-meteorological, (SAMT Publication, Tehran).

Nelson FE (1998). Cryoplanation terrace orientation in Alaska. *Geografiska Annaler Series A Physical Geography* **80**(2) 135–151.

Rich PM and Fu P (2000). Topoclimatic Habitat Models. *Proceedings of the Fourth International Conference on Integrating GIS and Environmental Modeling.*

Rich PM, Dubayah R, Hetrick WA and Saving SC (1994). Using View shed Models to Calculate Intercepted Solar Radiation: Applications in Ecology. *American Society for Photogrammetry and Remote Sensing Technical Papers* 524–529

Seif A, Solhi S and Solhi M (2014). Morphoradition Analysis western heights of Eghlid and its relationship with morphological changes. *Journal of Geography and Environmental Planning* **25**(4).

Trenhaile AS (1976). Cirque morphometry in the Canadian Cordillera. *Annals of the Association of American Geographers* **66** 451–462.